

## Onset and Near Threshold Evolution of the Cu $K\alpha$ X-Ray Satellites

M. Deutsch,<sup>1</sup> O. Gang,<sup>1</sup> K. Hämäläinen,<sup>2</sup> and C. C. Kao<sup>3</sup>

<sup>1</sup>Physics Department, Bar-Ilan University, Ramat-Gan 52900, Israel

<sup>2</sup>Physics Department, University of Helsinki, FIN-00014 Helsinki, Finland

<sup>3</sup>National Synchrotron Light Source, Brookhaven National Laboratory, Upton, New York 11973

(Received 27 November 1995)

The evolution of the Cu  $K\alpha_{3,4}$  spectrum is studied from threshold to saturation using synchrotron radiation photoexcitation. A pure shake-off behavior is observed, with a smooth and monotonic intensity rise from zero to saturation, confirming theoretical predictions. Different onset energies are observed for the spectral features, but the *shape* of the spectrum is found to be invariant for energies higher than 50 eV above threshold. Full-spectrum fits based on *ab initio* Dirac-Fock calculations and measured onset energies conclusively show the satellites to result from  $2p$  spectator transitions only, as predicted.

PACS numbers: 32.30.Rj, 32.70.-n, 32.80.Fb

Since they originate in multielectronic transitions, the near-threshold behavior of x-ray satellites can provide, in principle, important information on intershell and intra-shell electron correlations in atoms and on the excitation dynamics [1]. The threshold regions became accessible to detailed photoexcitation measurements only recently [2], with the advent of intense, tunable synchrotron x-ray sources. Even so, the slower development of more sophisticated optics, required at high energies, limited x-ray emission studies in these regions almost exclusively to soft x-rays and low-binding-energy valence satellites [3] in low- $Z$  atoms. These, however, are encumbered by numerous competing effects like initial- and final-state configuration interactions, interchannel coupling, solid state band-structure effects, etc., which make the elucidation of the basic single-atom shake-up and shake-off processes extremely difficult [1]. Armen *et al.* [4] demonstrated how the near-threshold Auger satellite emission spectrum can be employed to study the shake-up and shake-off processes separately. However, even this seminal study shows an  $\sim 25\%$  admixture of shake-up in the shake-off Auger line, prohibiting a full separation. The strong variation of the relative shake-off/shake-up probability with atomic and shell numbers, predicted by shake theory [5,6], provides a convenient way of separating these effects. Thus, the recent Be  $1s$  photoionization study of Krause and Caldwell [7] is a striking example of one limit: the predominance of (conjugate) shake-up, reaching an intensity of 40% of that of the single electron excitation. Armen *et al.*'s study explored the intermediate region, where the shake-up and shake-off are of the same order of magnitude. We present here a study of the other limit; the absolute predominance of the shake-off process [8]. This limit is achieved for inner-shell satellites in medium- $Z$  atoms, and was not hitherto studied. We chose to study the Cu  $K\alpha_{3,4}$  satellites, originating in  $2l$  electron shake processes accompanying  $1s$  photoionization. This choice of inner-shell satellites also eliminates solid state and nonlocalized band-structure effects dominating all previous valence-shell satellite stud-

ies. We confirm the theoretical prediction of the pure shake-off behavior of the spectrum, characterize the intensity and spectral shape behavior from threshold up, through the adiabatic [9] and intermediate energy regions up to the sudden approximation limit [5,6]. The different onset energies observed for the various spectral features indicate that the shape of the spectrum must vary with excitation energy near threshold. However, the lowest-energy measured spectrum, at  $\sim 50$  eV, is already fully developed, and for an additional range of  $\sim 1$  keV we find only a monotonic *intensity* increase to the sudden-approximation, high-energy limit, without any change in the spectral shape. The energy thresholds measured for the various features and the spectral shape clearly show the satellites to result from  $2p$  spectator transitions only. Full-spectrum fits based on *ab initio* relativistic Dirac-Fock (RDF) calculations allow assignment of the various features of the spectrum to specific transitions.

The measurements were carried out at the X25 wiggler beam line, NSLS, Brookhaven National Laboratory, with an experimental setup similar to that of Hämäläinen *et al.* [10]. A double crystal Si(220) monochromator with a bandpass of  $\sim 3$  eV and a flux of  $\sim 5 \times 10^{11}$  photons/sec was used. The sample was a polycrystalline high-purity Cu foil. The fluorescence spectrometer employed the Johann geometry with a 1 m diameter Rowland circle on a horizontal plane, and a spherically bent 3-in.-diameter Si(444) crystal providing  $\lesssim 1$  eV resolution. Incidence and the detection angles were fixed at  $45^\circ$ . This  $90^\circ$  scattering angle and the intrinsic Ge detector employed greatly reduced the background reaching the detector.

All spectra were corrected for self-absorption in the foil [11] and the small  $K\alpha$  photoexcitation efficiency energy dependence [12]. The highly sloping  $K\alpha_1$  contribution was stripped off by subtracting a Lorentzian tail fitted to the spectrum outside the energy range of the satellites. Care was taken to ensure that no satellite-related features were obliterated by these procedures. For further details see Ref. [13].

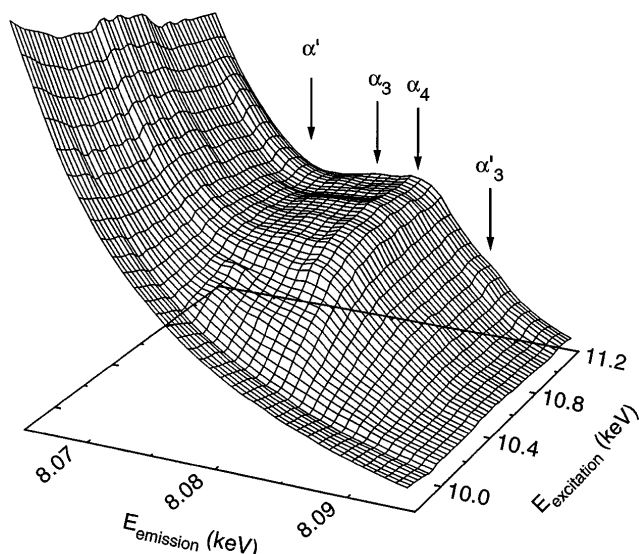


FIG. 1. Raw Cu  $K\alpha$  satellite spectra vs excitation energy near threshold. Note the high slope of the Cu  $K\alpha_1$  tail. The four underlying lines are marked by accepted notation.

The evolution of the spectra with excitation energy is shown in Fig. 1, along with the previously identified features. These were hitherto studied only for high-energy excitation in conventional x-ray tubes [14–16]. The most outstanding feature of the data is the smooth increase of the satellite complex intensity over a considerable energy range above threshold. This behavior is in marked contrast with the abrupt edgelike behavior observed in direct photoexcited *single-electron* emission spectra and with the accepted view of satellite spectra reaching saturation intensity within a few tens of eV above threshold [9].

A careful inspection of the corrected satellite spectra for all incident energies above 10 050 eV, the lowest energy above threshold where the spectrum could be measured with reasonable statistics, shows that the *shape* of all spectra are identical, within statistics. Furthermore, no energy shifts of the kind observed in subthreshold resonant Raman spectra [17] could be detected, to within  $\sim 1$  eV. The spectra differ only by an overall intensity factor, a plot of which is shown in Fig. 2. Since an abrupt intensity jump is predicted for shake-up at threshold while shake-off should increase smoothly from zero [1,4,5], the shape of the curve in Fig. 2 marks it as a pure shake-off process, unlike all previous near-threshold measurements where either comparable shake-up and shake-off [4], or almost pure (conjugate) shake-up [7] processes were found. This confirms a long-standing sudden-limit shake theory prediction of a fast increase in the relative shake-off/shake-up probability accompanying  $K$  ionization with decreasing  $n$ , the principal quantum number of the shake electron [8,18]. Recent RDF calculations yield off/up probability ratios of 0.40, 0.53, 3.1, and 10 for the respective  $4p$ ,  $4s$ ,  $3d$ , and  $3p$  shake electrons accompanying  $K$  ionization in Kr [8], and 0.4, 0.6, 6.9, and 8 for  $3p$ ,  $3s$ ,  $2p$ , and  $2s$  shake in Ar [18].

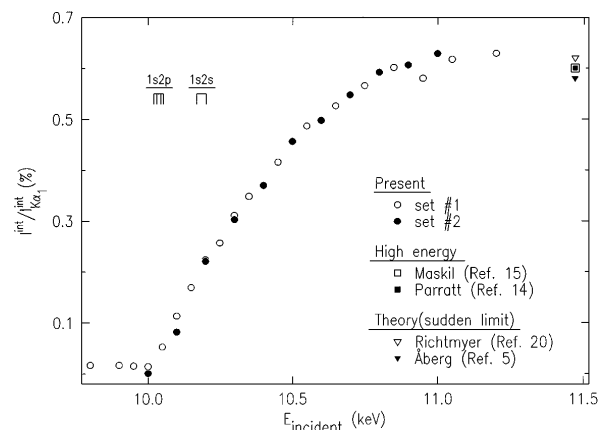


FIG. 2. Intensity of the satellite complex for varying incident exciting photon energy, measured with two different experimental resolutions (sets 1 and 2). The calculated RDF shake-off thresholds and the measured and theoretical high-energy limiting values are also shown.

While no similar values are available for copper, this trend points to a negligible,  $\leq 1\%$ , relative *shake-up* intensity in our case, which will not be observable in the present study. This conclusion is further supported by the onset measurements discussed below.

No slope changes or abrupt jumps are observed in Fig. 2 at the calculated  $1s2s$  threshold, indicating negligible contribution from  $2s$  spectator transitions. This is further supported by our line-shape fits below, and by a similar absence of  $ns$  spectator contributions in several other (mostly high-energy limit) studies [4,15,19]. This is most likely due to the very strong  $1s2s \rightarrow 1s2p3l$  Coster-Kronig transitions which depopulate the  $2s$  state very fast and should thus yield very broad and weak features [5,19].

Figure 2 also shows a surprisingly long saturation range;  $\sim 1$  keV, or  $\sim 10\%$  of the threshold energy. By comparison, the valence shell Auger shake-off satellite intensity of Ar [4], discussed above, levels off at  $\sim 70$  eV above threshold, or only  $\sim 2\%$  of the threshold energy. The saturation intensity,  $0.63\%$  of the  $K\alpha_1$  line, is in excellent agreement with the high-energy, x-ray-tube-measured intensity of  $0.60\%$  [14,16], and the sudden-approximation theoretical intensities of  $0.62\%$  [20] and  $0.58\%$  [5].

The fully developed emission spectrum is shown in Fig. 3. The four underlying lines are clearly distinguishable. To elucidate the origin of these lines we carried out *ab initio* RDF calculations using the GRASP code [21]. As usual [8,22], initial  $1s2l$  and final  $2s2l$  state wave functions ( $l = s, p$ ), were calculated in separate single-configuration runs, to allow for relaxation, and the transition energies obtained as differences of the relevant energy levels. The line strengths were calculated separately from the initial and final state wave functions, since the two separately generated sets are not orthogonal. The two results agree to better than  $5\%$  for all the lines in the figure. The results are shown as “stick diagrams” in Figs. 3(b) and 3(c). The

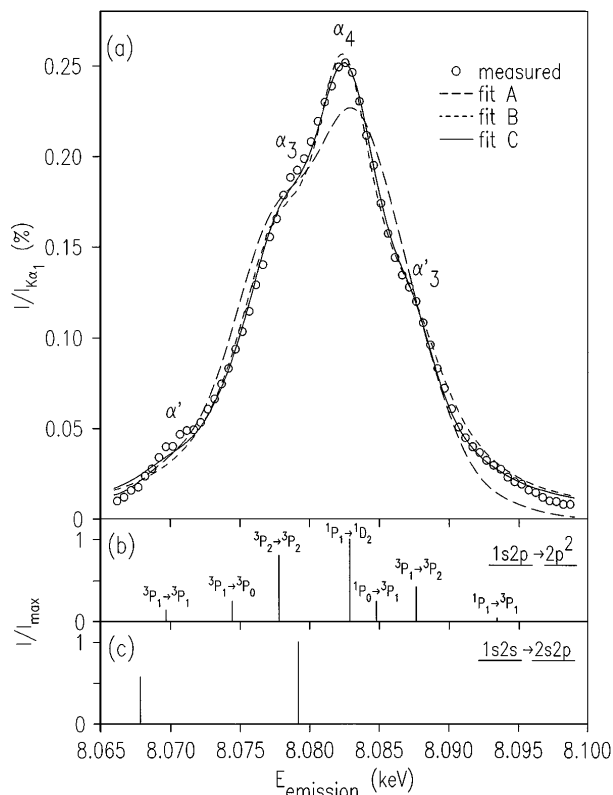


FIG. 3. (a) The fully developed measured satellite spectrum. The fits are based on the RDF calculated  $1s2p \rightarrow 2p^2$  transitions shown as a "stick diagram" in (b). Note the good agreement, in particular, for fits B and C. The lines in (b) are marked by the LS notation of their major constituents. The calculated  $1s2s \rightarrow 2s2p$  transitions are shown in (c).

$2p$  spectator lines are very well aligned with the measured spectrum. The maximal contribution of the  $2s$  multiplet is limited by the low intensity measured at the position of its second strongest line at 8067.5 eV. A model employing a Lorentzian representation for each line of the  $2p$  spectator multiplet was fitted to the data, following three progressively less constrained procedures. In fit A equal widths were assumed for all lines and only this width, an intensity scale factor, and a relative shift between the energy scales of the measurements and the calculations ( $\sim 1$  eV) were refined in the fit. In fit B the equal width restriction was removed, but the relative integrated intensities of the lines were fixed at the calculated value. In fit C even this last restriction was removed. As can be seen, even the most constrained fit A yields to a reasonable agreement with the measured data. The fit becomes excellent for B, demonstrating the high accuracy of the single-configuration RDF method even for such highly correlated shake-off transitions. It also allows a clear assignment of the features of the measured spectrum to calculated  $2p$  spectator transitions, as marked on Fig. 3(b). Attempts to include the  $2s$  spectator transitions in the fit invariably resulted in a vanishingly small intensity for this multiplet, corroborating the conclusions above.

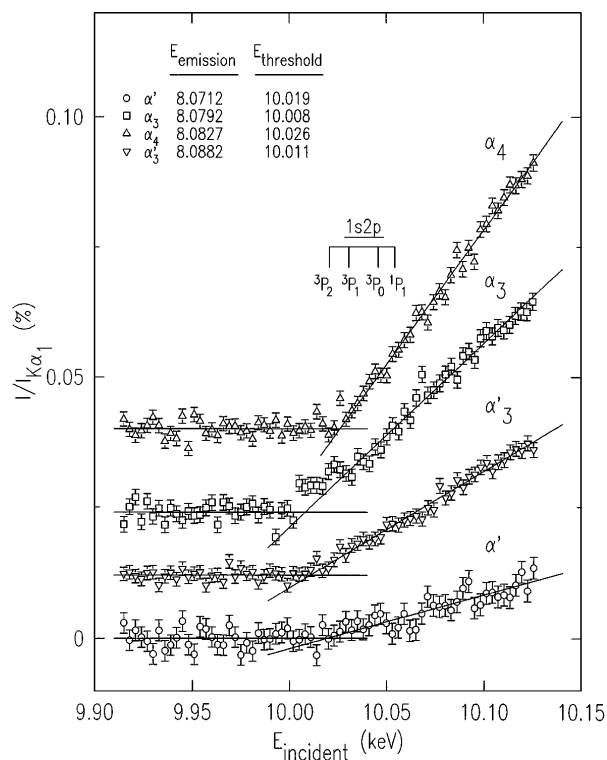


FIG. 4. Fluorescence intensity scans at the indicated emission energies near threshold. The curves are shifted relative to each other for clarity. The solid lines are fits to the data below 10 000 and above 10 050 eV, respectively. The intersections are taken as the thresholds for the corresponding features. Note the smooth rise of the intensity from zero, the different threshold energies, and the overall agreement with the RDF-calculated  $1s2p$  levels.

To determine the onset energy of the features marked in Fig. 3, the spectrometer was kept fixed at each of the relevant emission energies in turn, and the incident excitation energy scanned through the threshold region. The resultant curves are shown in Fig. 4. Strikingly, even on this magnified scale, no edgeline intensity jumps appear in the data, strongly supporting our previous conclusion of a shake-off origin for the satellites. The similar trend in the valence-shell shake-off Auger satellites of argon, observed by Armen *et al.* [4], was, however, largely obscured by an admixture of discreet *shake-up*  $3p \rightarrow np$  ( $n = 5, 6, \dots$ ) contributions so that a discreet  $\sim 25\%$  jump (of the saturated shake-off intensity) is observed at threshold. Furthermore, while at high energies the shake-off is found in that study to dominate over the shake-up by a factor of 2; near threshold the total Auger satellite yield is dominated by *shake-up* processes. By contrast, here Fig. 4 demonstrates a smooth rise for all lines, and hence a pure shake-off process.

Figure 4 also shows different thresholds for the different lines. Those of the  $\alpha_3$  and  $\alpha_4$  lines differ by  $\sim 20$  eV, commensurate with the  $2p_{1/2}-2p_{3/2}$  subshell energy separation. The weaker features,  $\alpha'$  and  $\alpha'_3$ , seem to be associated with the  $\alpha_4$  and  $\alpha_3$  lines, correspondingly, although

their thresholds are downshifted and upshifted from those of these lines by a few eV. Considerably better statistics will be required, however, to determine such small energy shifts with confidence. The RDF-calculated  $1s2p$  levels, shown in the figure, should correspond to the measured thresholds through the transition assignments of Fig. 3, of which these levels are the initial states. The overall agreement in Fig. 4 with the measured thresholds is indeed reasonable, although minor discrepancies exist. For example, an  $\sim 10$  eV shift between the calculated and measured energy scales is found. Also, the calculated  $^3P_2-^1P_1$  difference of 25 eV is somewhat larger than the corresponding  $\alpha_3 - \alpha_4$  threshold difference of 18 eV. The  $\alpha'$  and  $\alpha_3$  thresholds are in between those of  $\alpha_3$  and  $\alpha_4$ , as expected from their initial state assignments to the  $^3P_1$  level. They are, however, too weak to support a meaningful quantitative comparison with the calculations. These discrepancies are not surprising in view of the simplified, fully relaxed, single-configuration calculations. More sophisticated multichannel-multiconfiguration calculations will be required to reproduce the thresholds more accurately.

In conclusion, we presented here a study of the near-threshold evolution of a pure shake-off satellite spectrum, unencumbered by admixture with shake-up processes and/or solid state, band-structure effects. Line assignments were based on full-spectrum fits using RDF calculations, and on onset energies of the various spectral features. Several long-standing general predictions concerning single photon–two electron excitations were confirmed, including the strong increase of the relative shake-off/shake-up ratio in inner shells and the continuous increase from zero of the shake-off probability. Most importantly, the study revealed a striking two-regime behavior. In the first, extending to 50 eV from threshold, individual shake channels open at different energies and the line shape must, therefore, undergo *shape* as well as *intensity* variations. The shape variations, however, saturate very fast, since the line shape for 10 050 eV is already fully developed and measured to be identical to those at higher energies. In the second regime, extending from  $\sim 10\,050$  to  $\sim 11\,000$  eV, only the overall *intensity* of the spectrum changes, increasing monotonically and smoothly to a saturation value slightly above the high-energy limit. This study concentrated mostly on the second regime. Further measurements, much more demanding technically, are planned to elucidate the details of the spectral evolution in the first regime.

Discussions with and expert advice by T. Åberg and L. E. Berman are gratefully acknowledged. This work is supported by the German-Israeli Binational Science Foundation, and the U.S. DOE under Contract No. DE-

AC02-76CH00016. K. H. is indebted to the Finnish Academy for financial support (Contract No. 8582).

- 
- [1] B. Crasemann, J. Phys. (Paris), Colloq. **48**, C9-389 (1987); V. Schmidt, Rep. Prog. Phys. **55**, 1483 (1992).
  - [2] R. D. Deslattes, R. E. LaVilla, P. L. Cowan, and A. Henins, Phys. Rev. A **27**, 923 (1983).
  - [3] N. Wassdahl *et al.*, Phys. Rev. Lett. **64**, 2807 (1990); Y. Ma, K. E. Miyano, P. L. Cowan, Y. Aglitzkiy, and B. A. Carlin, *ibid.* **74**, 478 (1995).
  - [4] G. B. Armen *et al.*, Phys. Rev. Lett. **54**, 182 (1985).
  - [5] T. Åberg, in *Proceedings of the International Conference on Inner-Shell Ionization Phenomena and Future Applications*, edited by R. W. Fink, S. T. Manson, J. M. Palms, and P. V. Rao, U.S. AEC Report No. CONF-720404 (NTIS, U.S. Dept. of Commerce, Springfield, VA, 1972), p. 1509.
  - [6] J. Tulkki and T. Åberg, J. Phys. B **18**, L489 (1985); J. Tulkki *et al.*, Z. Phys. D **5**, 241 (1987).
  - [7] M. O. Krause and C. D. Caldwell, Phys. Rev. Lett. **59**, 2736 (1987).
  - [8] D. L. Wark *et al.*, Phys. Rev. Lett. **67**, 2291 (1991); S. J. Schaphorst *et al.*, Phys. Rev. A **47**, 1953 (1993).
  - [9] J. Stöhr, R. Jaeger, and J. J. Rehr, Phys. Rev. Lett. **51**, 821 (1983); T. D. Thomas, Phys. Rev. Lett. **52**, 417 (1984); E. Vatai, Phys. Rev. **38**, 3777 (1988).
  - [10] K. Hämäläinen, D. P. Siddons, J. B. Hastings, and L. E. Berman, Phys. Rev. Lett. **67**, 2850 (1991).
  - [11] E. P. Bertin, *Introduction to X-Ray Spectrometric Analysis* (Plenum, New York, 1978), p. 373.
  - [12] *International Tables for X-ray Crystallography*, edited by C. H. MacGillavry and G. D. Rieck (Kynoch, Birmingham, 1968), Vol. III, p. 161.
  - [13] M. Deutsch, O. Gang, K. Hämäläinen, and C. C. Kao (to be published).
  - [14] L. G. Parratt, Phys. Rev. **50**, 1 (1936); H. J. Edwards and J. I. Langford, J. Appl. Crystallogr. **4**, 43 (1971).
  - [15] A. Li-Scholz, A. Leiberich, and W. Scholz, Phys. Rev. A **26**, 3232 (1982).
  - [16] N. Maskil and M. Deutsch, Phys. Rev. A **38**, 3467 (1988).
  - [17] P. Eisenberger, P. M. Platzman, and H. Winick, Phys. Rev. Lett. **36**, 623 (1976); T. Åberg and B. Crasemann, in *Resonant Anomalous X-Ray Scattering*, edited by G. Materlik, C. J. Sparks, and K. Fischer (Elsevier, Amsterdam, 1994).
  - [18] K. G. Dyall, J. Phys. B **16**, 3137 (1983); see also discussion and references in T. Mukoyama and Y. Ito, Nucl. Instrum. Methods Phys. Res., Sect. B **87**, 26 (1994).
  - [19] M. Deutsch *et al.*, Phys. Rev. A **51**, 283 (1995).
  - [20] R. D. Richtmyer, Phys. Rev. **49**, 1 (1936).
  - [21] K. G. Dyall *et al.*, Comput. Phys. Commun. **55**, 425 (1989).
  - [22] See discussion and references in Ref. [19].